Inorg. Chem. **2004**, *43*, 309–316

Mechanism of the Axial Ligand Substitution Reactions on the Head-to-Tail α-Pyridonato-Bridged *cis*-Diammineplatinum(III) Dinuclear Complex with Olefins

Moritatsu Arime,[†] Koji Ishihara,*[,†] and Kazuko Matsumoto*[,‡]

Department of Chemistry, School of Science and Engineering, Waseda University, Okubo, Shinjuku-ku, Tokyo 169-8555, Japan

Received May 31, 2003

Reactions of the head-to-tail α-pyridonato-bridged *cis*-diammineplatinum(III) dinuclear complex having equivalent two platinum atoms, $Pt(N_3O)$, with *p*-styrenesulfonate and 4-penten-1-ol were studied kinetically. Under the pseudo first-order reaction conditions in which the concentration of the Pt^{III} dinuclear complex is much smaller than that of olefin, a consecutive basically four-step reaction was observed for the reaction with *p*-styrenesulfonate, but for the reaction with 4-penten-1-ol, the reaction was three step. The olefin π-coordinates to one of the two equivalent Pt atoms in the first step (step 1), followed by the second π-coordination of another olefin molecule to the other Pt atom (step 2). In the next step (step 3), the nucleophilic attack of water to the first π-coordinated olefin initiates its $\pi-\sigma$ bond conversion on the Pt atom, and the second π-bonding olefin molecule on the other Pt atom is released. Finally, dissociation of the alkyl group on the $Pt(N_3O)$ and reduction of the Pt^{III} dinuclear complex to the Pt^{II} dinuclear complex occur (step 4). The first water substitution with olefin (step 1) consists of two paths, the reaction of the diaqua dimer complex (path a) and the reaction of the aquahydroxo dimer complex (path b), whereas the second substitution (step 2) proceeds through three reaction paths: the normal path of the direct substitution of H_2O (path c), the path of the coordinated OH^- substitution (path d), and the path via the coordinatively unsaturated five-coordinate intermediate (path e). The reaction with *p*-styrenesulfonate proceeds through paths c, d, and e, whereas the reaction with 4-penten-1-ol proceeds through paths c and d. The third step (step 3) for the reaction with *p*-styrenesulfonate involves the coordinatively unsaturated intermediate, but that for the 4-pentene reaction does not. The reactivities of the HH dimer and HT dimer with olefins are compared and discussed.

Introduction

Amidato-bridged Pt^{III} dinuclear complexes $[(L)Pt(NH_3)_2(\mu\text{-amidato})_2Pt(NH_3)_2(L)]^{n+}$ (amidato = α-pyridonato, α-pyrrolidonato, or pivalamidato, L = NO_3^-, NO_2^-, H_2O, Cl^-, or Br^-) having a metal−metal bonding sometimes exist in two forms, head-to-head (HH) and head-to-tail (HT),[1] as shown in Chart 1. The HH isomer is formed by oxidation of the mixed valent "platinum blues".[1−11] The two platinum atoms in the HH complexes are not equivalent: one is ligated by two ammine nitrogen atoms and two amidate oxygen atoms ($Pt(N_2O_2)$), whereas the other is by four nitrogen atoms ($Pt(N_4)$). In the HT complexes, the two platinum atoms are equivalent ($Pt(N_3O)$).

* To whom correspondence should be addressed. E-mail: ishi3719@waseda.jp (K.I.) and kmatsu@waseda.jp (K.M.).

[†] Materials Research Laboratory for Bioscience and Photonics, Graduate School of Science and Engineering, Waseda University.

[‡] Advanced Research Institute for Science and Engineering, Waseda University.

(1) Hollis, L. S.; Lippard, S. J. *Inorg. Chem.* **1983**, *22*, 2605.
(2) Bryan, S.; Dickson, M. K.; Roundhill, D. M. *Inorg. Chem.* **1987**, *26*, 3878 and references therein.
(3) Faggiani, R.; Lippert, B.; Lock, C. J. L.; Speranzini, R. A. *J. Am. Chem. Soc.* **1981**, *103*, 1111.
(4) El-Mehdawi, R.; Bryan, S. A.; Roundhill, D. M. *J. Am. Chem. Soc.* **1985**, *107*, 6282 and references therein.
(5) Hollis, L. S.; Roberts, M. M.; Lippard, S. J. *Inorg. Chem.* **1983**, *22*, 3637.
(6) O'Halloran, T. V.; Roberts, M. M.; Lippard, S. J. *Inorg. Chem.* **1986**, *25*, 957.
(7) Lippert, B.; Schoellhorn, H.; Thewalt, U. *Inorg. Chem.* **1986**, *25*, 407.
(8) Schoellhorn, H.; Eisenmann, P.; Thewalt, U.; Lippert, B. *Inorg. Chem.* **1986**, *25*, 3384.
(9) Lippert, B.; Schoellhorn, H.; Thewalt, U. *J. Am. Chem. Soc.* **1986**, *108*, 525.
(10) (a) Abe, T.; Moriyama, H.; Matsumoto, K. *Chem. Lett.* **1989**, 1857. (b) Abe, T.; Moriyama, H.; Matsumoto, K. *Inorg. Chem.* **1991**, *30*, 4198.
(11) Matsumoto, K.; Sakai, K. *Adv. Inorg. Chem.* **2000**, *49*, 375.

10.1021/ic034599q CCC: $27.50
Published on Web 12/05/2003

Chart 1

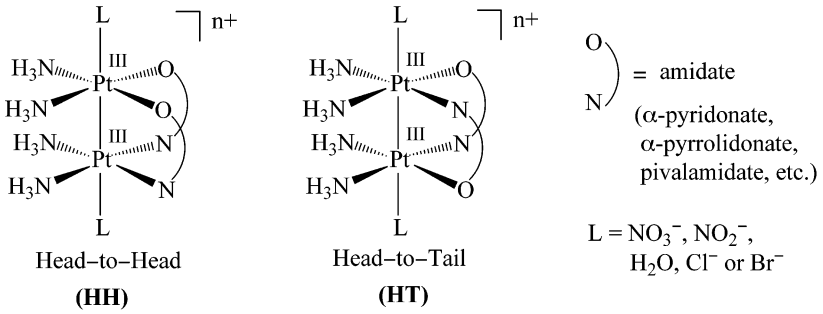

It is known that the HH amidato-bridged Pt^{III} dinuclear complexes act as catalysts for the oxidation of olefins to aldehydes, ketones, epoxides, and α,*β*-diols.[12−15] Several alkyl Pt^{III} dinuclear complexes have been synthesized by the reactions of the HH complexes with olefins, and their crystal structures have been determined by X-ray crystallography.[13] We have studied kinetically the reactions of the HH α-pyridonato-bridged Pt^{III} dinuclear complex with some olefins and an alkyne, such as *p*-styrenesulfonate, 2-methyl-2-propene-1-sulfonate, 4-penten-1-ol, and 4-pentyn-1-ol, to clarify the formation mechanism of the alkyl Pt^{III} dinuclear complexes, and proposed the reaction mechanism as shown in Scheme S1 (Supporting Information).[16] The reactions proceed as a consecutive three-step or four-step reaction. The olefin π-coordinates preferentially to the $Pt(N_2O_2)$ in the first step, followed by the second π-coordination of another olefin molecule to the $Pt(N_4)$ in the second step. In the third step, the nucleophilic attack of a water molecule to the coordinated olefin causes the $\pi-\sigma$ bond conversion on the $Pt(N_2O_2)$ to form the σ-complex, and the second π-bonding olefin molecule on the $Pt(N_4)$ is released. The β-hydroxy σ-complex is not stable, and in the fourth step, the alkyl group on the $Pt(N_2O_2)$ is liberated as the ketonyl compound, and the Pt^{III} dinuclear complex is reduced to the Pt^{II} dinuclear complex. We have also reported previously the kinetic and equilibrium studies of the axial aqua ligand substitution with halide in the HH and HT α-pyridonato-bridged dinuclear complexes in order to examine the difference in reactivity of the two isomers.[17,18] Further, we have recently studied the axial ligand substitution with halide ions in the HH α-pyrrolidonato-bridged Pt^{III} dinuclear complex and the HH pivalamidato-bridged Pt^{III} dinuclear complex, to examine the effect of the bridging ligand on the axial ligand substitution.[19] Substantial difference in the axial reactivity was found for the HH and HT α-pyridonato-bridged dinuclear complexes. The axial substitution reactivity also varied depending on the bridging ligand in the HH Pt^{III} dinuclear complexes.

In this paper, we examine the reaction mechanism of the α-pyridonato-bridged HT Pt^{III} dinuclear complex $[(H_2O)(NH_3)_2Pt(\mu\text{-}C_5H_4NO)_2Pt(NH_3)_2(H_2O)]^{4+}$, and compare the reactivity of the HH and HT dinuclear complexes toward olefins. *p*-Styrenesulfonate and 4-penten-1-ol were selected as olefins, because these olefins show considerably different reaction patterns toward the HH α-pyridonato-bridged Pt^{III} dinuclear complex.[16]

Results and Discussion

Reaction with Sodium *p*-Styrenesulfonate. The reaction of the HT dimer with sodium *p*-styrenesulfonate gives sodium *p*-acetylbenzenesulfonate and the Pt(II) dimer complex as shown in eq 1. The time course changes in UV−vis

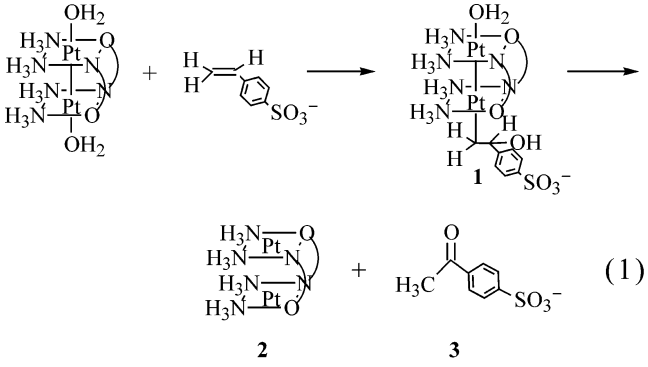

(1)

absorption spectra under the pseudo first-order conditions, $C_{HH} \ll C_L$ (Figures S1a and S2a, Supporting Information), were almost the same as those observed for the HH α-pyridonato-bridged dimer reaction.[16] The present reaction consists of four steps (Figures S1b and S2b): the fastest step (step 1), two intermediate steps (steps 2 and 3), and the slowest step (step 4). Steps 1−3 were first-order reactions, whereas step 4 was very slow and deviated from the first-order reaction curvature after prolonged reaction time, so the rate constant for step 4 could not be determined. The pseudo first-order rate constants, k_{obs1}, k_{obs2}, and k_{obs3} for steps 1−3, respectively, were dependent on both the excess ligand concentration (C_L) and $[H^+]$ as shown in Figure 1. It is worthy of note that k_{obs2} for the present system is different

(12) Matsumoto, K.; Mizuno, K.; Abe, T.; Kinoshita, J.; Shimura, H. *Chem. Lett.* **1994**, 1325.
(13) Matsumoto, K.; Nagai, Y.; Matsunami, J.; Mizuno, K.; Abe, T.; Somazawa, R.; Kinoshita, J.; Shimura, H. *J. Am. Chem. Soc.* **1998**, *120*, 2900.
(14) Lin, Y.-S.; Takeda, S.; Matsumoto, K. *Organometallics* **1999**, *18*, 4897.
(15) Matsumoto, K.; Sakai, K. *Adv. Inorg. Chem.* **1999**, *49*, 375.
(16) Saeki, N.; Nakamura, N.; Ishibashi, T.; Arime, M.; Sekiya, H.; Ishihara, K.; Matsumoto, K. *J. Am. Chem. Soc.* **2003**, *125*, 3605.
(17) Saeki, N.; Hirano, Y.; Sasamoto, Y.; Sato, I.; Toshida, T.; Ito, S.; Nakamura, N.; Ishihara, K.; Matsumoto, K. *Bull. Chem. Soc. Jpn.* **2001**, *74*, 861.
(18) Saeki, N.; Hirano, Y.; Sasamoto, Y.; Sato, I.; Toshida, T.; Ito, S.; Nakamura, N.; Ishihara, K.; Matsumoto, K. *Eur. J. Inorg. Chem.* **2001**, 2081.
(19) Shimazaki, K.; Sekiya, H.; Ishihara, K.; Matsumoto, K. *Eur. J. Inorg. Chem.* **2003**, 1785.

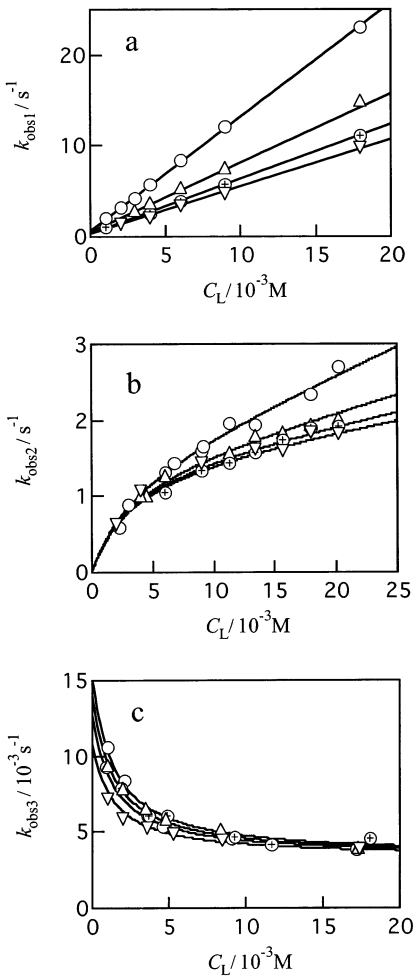

Figure 1. Dependence of the observed rate constants on C_L for the reaction of the HT dimer with *p*-styrenesulfonate at $I = 2.0$ M. (a) For step 1, at 25 °C and $[H^+]/M = 0.412$ (○), 0.824 (△), 1.23 (⊕), 1.64 (▽). (b) For step 2, at 25 °C and $[H^+]/M = 0.412$ (○), 0.824 (△), 1.24 (⊕), 1.65 (▽). (c) For step 3, at 40 °C and $[H^+]/M = 0.0401$ (○), 0.401 (⊕), 0.803 (△), 1.61 (▽).

from that for the HH α-pyridonato-bridged dimer reaction;[16] in the latter reaction, the k_{obs2} was dependent on C_L similarly to Figure 1b, but was independent of $[H^+]$.

For the HH dimer in Scheme S1, the first ligand substitution with olefin occurs to the $Pt(N_2O_2)$, and the first deprotonation of the aqua ligand occurs to the $H_2O-Pt(N_4)$ exclusively (step 1). The second substitution takes place on the $Pt(N_4)$ (step 2). The π-bond ⇄ σ-bond conversion occurs in step 3, which takes place on the $Pt(N_2O_2)$.[13,20,21] At step 4, the intramolecular reaction proceeds and the Pt^{III} complex is reduced to the HH Pt^{II} dinuclear complex to release the ketone.

A similar reaction scheme can be drawn for step 1 in the present HT dimer reaction as shown in Scheme 1; however, different from the corresponding reaction of the HH complex, the path $k_2^{\#}$ is added in Scheme 1, which was also observed in the reaction of the present HT complex with Cl^-.[18] This route comes from the k_{obs2} dependence on $[H^+]$ as well as on C_L.

The experimental data in Figure 1 give eq 2 for k_{obs1}, and eq 3 is derived from the reaction paths in Scheme 1.

$$k_{obs1} = k_{f1}C_L + k_{d1} \tag{2}$$

$$k_{obs1} = \frac{k_1 + \dfrac{k_1^{\#}K_{h1}}{[H^+]}}{1 + \dfrac{K_{h1}}{[H^+]}}[L] + \frac{k_{-1} + \dfrac{k_{-1}^{\#}K_{h2}}{[H^+]}}{1 + \dfrac{K_{h2}}{[H^+]}} \tag{3}$$

Equations 4 and 5 are obtained from eqs 2 and 3, under the present pseudo first-order condition, $C_{HH} \ll C_L$. The values k_{f1} and k_{d1} are the rate constants of the forward and the reverse reactions of step 1 in Scheme 1, respectively.

$$k_{fl} = \frac{k_1 + \dfrac{k_1^{\#}K_{h1}}{[H^+]}}{1 + \dfrac{K_{h1}}{[H^+]}} \tag{4}$$

The plot of $k_{f1}(1 + K_{h1}/[H^+])$ vs $[H^+]^{-1}$ was linear (Figure S3a, Supporting Information). In the denominator of eq 5, $K_{h2}/[H^+]$ is negligible compared to unity under the present conditions, since the plot of k_d vs $[H^+]^{-1}$ (Figure S3b) is linear within the experimental errors.

$$k_{dl} = \frac{k_{-1} + \dfrac{k_{-1}^{\#}K_{h2}}{[H^+]}}{1 + \dfrac{K_{h2}}{[H^+]}} \approx k_{-1} + \frac{k_{-1}^{\#}K_{h2}}{[H^+]} \tag{5}$$

On the other hand, k_{obs2} for step 2 in Scheme 1 is expressed as eq 6, when the steady-state approximation is applied to the coordinatively unsaturated complex.

$$k_{obs2} = \frac{k_2 + \dfrac{k_2^{\#}K_{h2}}{[H^+]}}{1 + \dfrac{K_{h2}}{[H^+]}}[L] + \frac{\dfrac{k_3k_4[H^+]}{[H^+] + K_{h2}}[L] + k_{-3}k_{-4}}{k_4[L] + k_{-3}} \approx \left(k_2 + \frac{k_2^{\#}K_{h2}}{[H^+]}\right)[L] + \frac{k_3[L]}{[L] + k_{-3}/k_4} \tag{6}$$

The change of the ^1H NMR spectra (Figure S4, Supporting Information) for the present *p*-styrenesulfonate system was quite similar to that for the HH dimer system,[16] i.e., the formation of the σ-complex **1** (step 3 in Scheme 1, eq 1) was followed by the liberation of the ketone **3** from the σ-complex and the reduction of the σ-complex to the HT α-pyridonato-bridged Pt^{II} dinuclear complex **2** (step 4).

The reactive intermediate having the unsaturated coordination site at step 3 in Scheme 1 is necessary to explain the drastic decrease of k_{obs3} with increasing C_L (Figure 1c). Equation 7 is derived when the steady-state approximation

(20) Matsumoto, K.; Matsunami, J.; Mizuno, K.; Uemura, H. *J. Am. Chem. Soc.* **1996**, *118*, 8959.
(21) Sakai, K.; Tanaka, Y.; Tsuchiya, Y.; Hirata, K.; Tsubomura, T.; Iijima, S.; Bhattacharjee, A. *J. Am. Chem. Soc.* **1998**, *120*, 8366.

Scheme 1. Mechanism for the Reaction of the HT Dimer with Sodium *p*-Styrenesulfonate

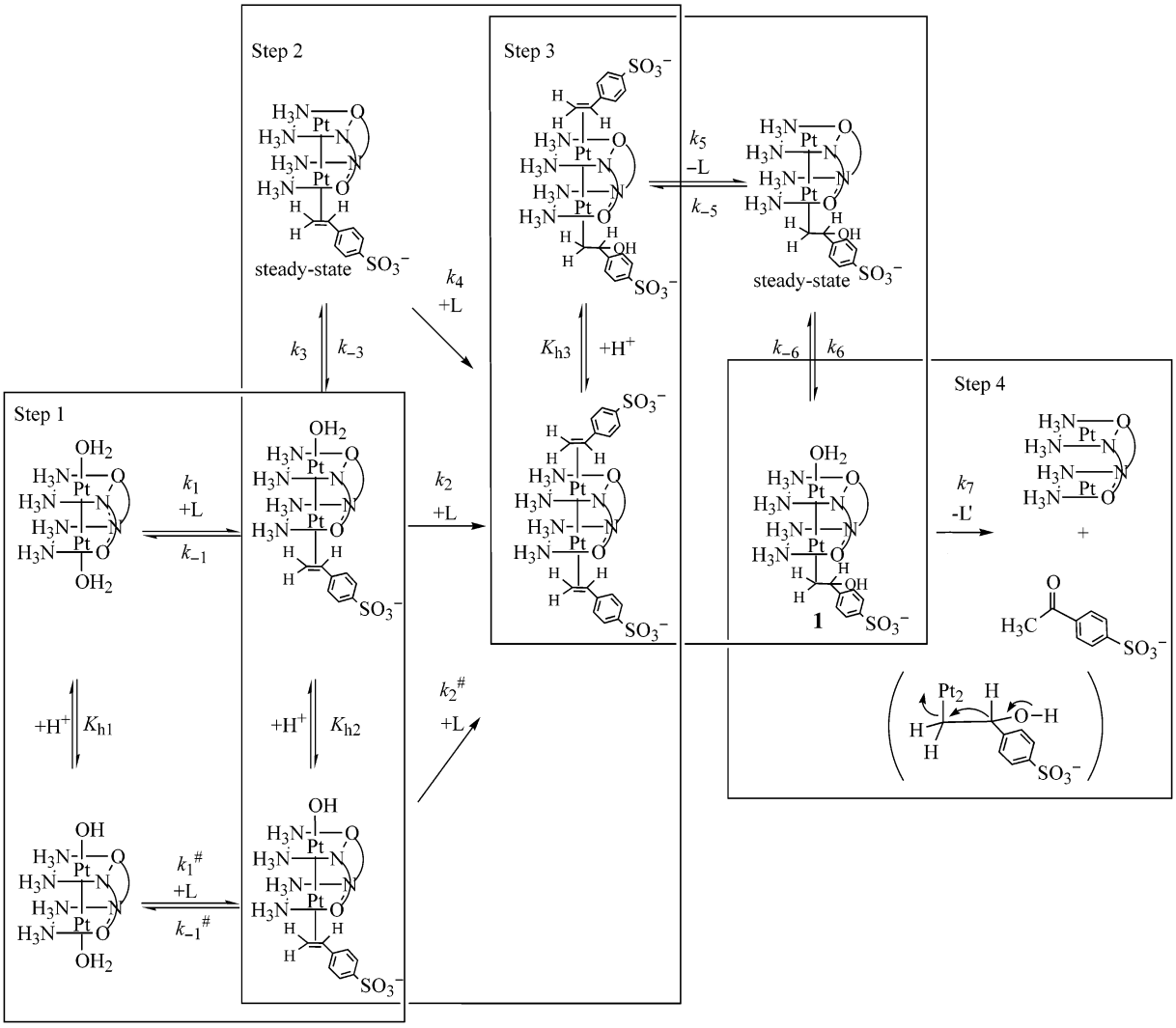

is applied to the intermediate at step 3 in Scheme 1. This equation agrees with the experimental data as shown in Figure 1c.

$$k_{obs3} = \frac{\dfrac{k_5 K_{h3}}{[H^+] + K_{h3}} + \dfrac{k_{-5}k_{-6}[L]}{k_6}}{\dfrac{k_{-5}[L]}{k_6} + 1} \qquad (7)$$

The best-fit curves in Figure 1 were drawn by applying a non-linear least-squares fitting of eqs 3, 6, and 7 to the experimental data, and agree well with the experimental results. All the rate constants in these equations were calculated by using $K_{h1} = 1.05 \times 10^{-2}$ M (25 °C, $I = 2.0$ M) determined previously,[18] and are tabulated in Table 1.

Reaction with 4-Penten-1-ol. The reaction with 4-penten-1-ol gave the σ-complex **4** as the final product as shown in eq 8. The complex is stable under the experimental conditions, and does not release the alkyl group. The formation of the σ-complex was confirmed by the ^{1}H NMR spectrum (Figure S5, Supporting Information). The peaks of the bridging α-pyridonato ligand in the unreacted Pt^{III} dinuclear complex, those of the reacted Pt^{III} dinuclear complex (σ-complex), and those of the tetrahydrofurfuryl protons of the σ-complex were observed. The structure of the σ-complex is analogous to that of the previously reported pivalamidato-bridged 2-methyl tetrahydrofurfuryl complex, whose structure was elucidated by X-ray crystallography.[13]

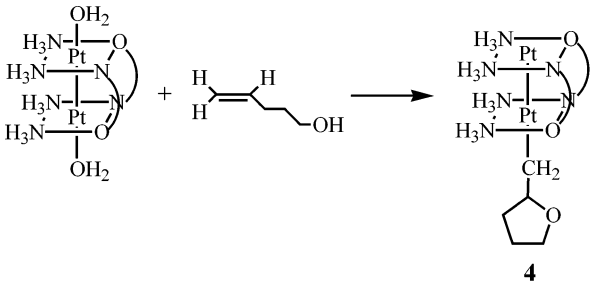

(8)

4

A three-step reaction was observed under the pseudo first-order conditions ($C_{HH} \ll C_L$) (Figure 2). Step 1 was fast and could not be detected even at lower temperature for the HH dimer reaction with 4-penten-1-ol,[16] whereas for the present HT dimer reaction, the last part of step 2 could be detected at lower C_L (Figure 2b,d), but the C_L dependence of the rate

Scheme 2. Mechanism for the Reaction of the HT Dimer with 4-Penten-1-o1

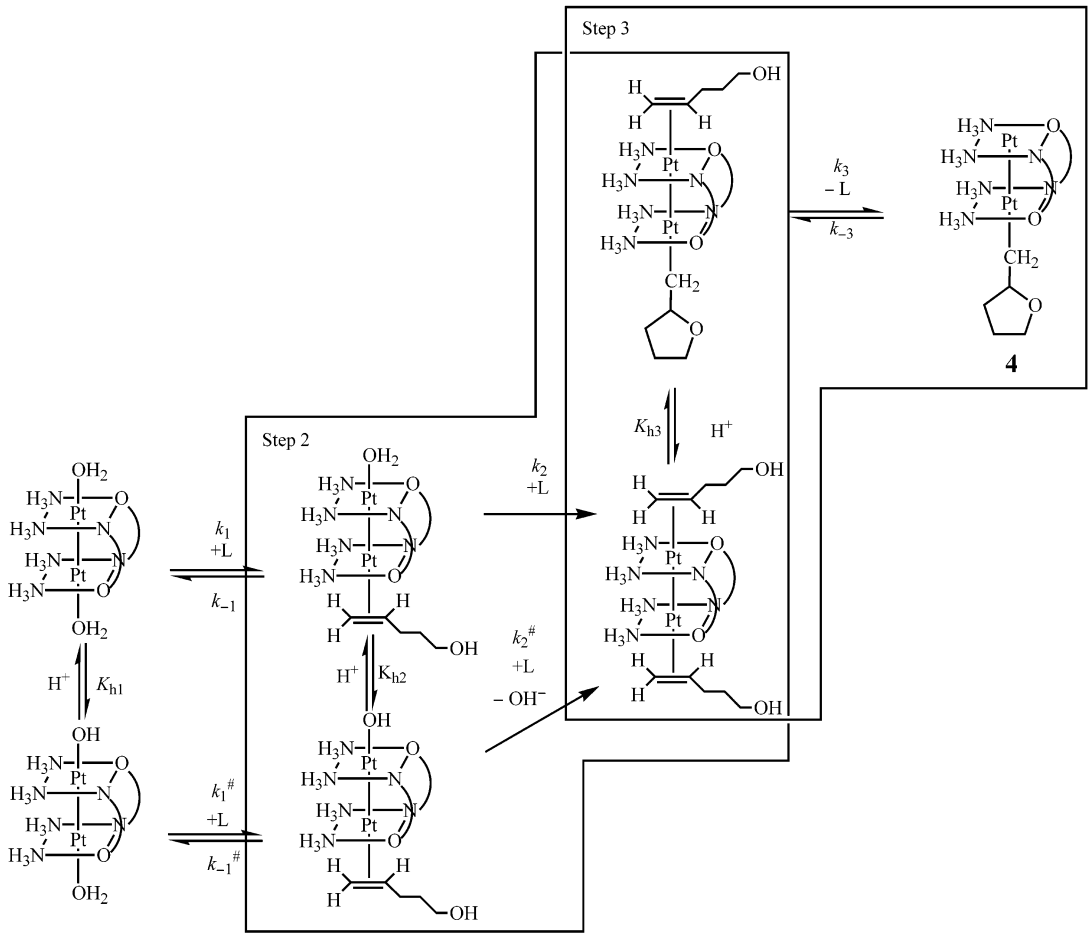

Table 1. The Rate and Equilibrium Constants (25 °C, I = 2.0 M) for the Reactions of the HH and HT α-Pyridonato-Bridged Pt^{III} Dinuclear Complexes with Olefins

p-styrenesulfonate			4-penten-1-ol		
HH[a]	HT[b]	HT[c]	HH[a]	HT[b]	HT[c]
		Step 1			
$k_1 = 1.3 \times 10^3\ M^{-1}\ s^{-1}$	$k_1 = 2.3 \times 10^2\ M^{-1}\ s^{-1}$	$k_1 = 1.2 \times 10^2\ M^{-1}\ s^{-1}$			
$k_1^{\#} = 4.4 \times 10^3\ M^{-1}\ s^{-1}$	$k_1^{\#} = 4.3 \times 10^4\ M^{-1}\ s^{-1}$	$k_1^{\#} = 2.2 \times 10^4\ M^{-1}\ s^{-1}$			
$k_{-1} = 0.90\ s^{-1}$	$k_{-1} = 0.19\ s^{-1}$	$k_{-1} = 0.10\ s^{-1}$			
$k_{-1}^{\#} = 2.3 \times 10^2\ s^{-1}$	$k_{-1}^{\#} = 26\ s^{-1}$	$k_{-1}^{\#} = 13\ s^{-1}$			
$K_{h2} = 3.8 \times 10^{-4}$ M	$K_{h2} = 7.7 \times 10^{-3}$ M	$K_{h2} = 7.7 \times 10^{-3}$ M			
		Step 2			
$k_2 = 31 \pm 3\ M^{-1}\ s^{-1}$	$k_2 = 17 \pm 5\ M^{-1}\ s^{-1}$	$k_2 = 8.5\ M^{-1}\ s^{-1}$	$k_2 = 29\ M^{-1}\ s^{-1}$	$k_2 = 20\ M^{-1}\ s^{-1}$	$k_2 = 10\ M^{-1}\ s^{-1}$
	$k_2^{\#} = (2.8 \pm 0.4) \times 10^3\ M^{-1}\ s^{-1}$	$k_2^{\#} = 1.4 \times 10^3\ M^{-1}\ s^{-1}$	$k_2^{\#} = 6.2 \times 10^4\ M^{-1}\ s^{-1}$	$k_2^{\#} = 2.4 \times 10^3\ M^{-1}\ s^{-1}$	$k_2^{\#} = 1.2 \times 10^3\ M^{-1}\ s^{-1}$
$k_3 = 0.64 \pm 0.06\ s^{-1}$	$k_3 = 1.4 \pm 0.1\ s^{-1}$	$k_3 = 0.7\ s^{-1}$	$K_{h2} = 6.3 \times 10^{-3}$ M	$K_{h2} = 2.0 \times 10^{-3}$ M	$K_{h2} = 2.0 \times 10^{-3}$ M
$k_{-3}/k_4 = 4.0 \times 10^{-3}$ M	$k_{-3}/k_4 = 3.2 \times 10^{-3}$ M	$k_{-3}/k_4 = 3.2 \times 10^{-3}$ M			
		Step 3			
$k_5 = 3.7 \times 10^{-3}\ s^{-1}$	$k_5 = 1.6 \times 10^{-2}\ s^{-1}$ [d]	$k_5 = 8.0 \times 10^{-3}\ s^{-1}$ [d]	$k_{-3} = 44\ M^{-1}\ s^{-1}$	$k_{-3} = 5.0\ M^{-1}\ s^{-1}$	$k_{-3} = 2.5\ M^{-1}\ s^{-1}$
$K_{h3} = 0.21$ M	$K_{h3} = 3.63$ M[d]	$K_{h3} = 3.63$ M[d]	$k_3 = 1.2\ s^{-1}$		
$k_{-6} = 5.4 \times 10^{-4}\ s^{-1}$	$k_{-6} = 3.3 \times 10^{-3}\ s^{-1}$ [d]	$k_{-6} = 1.7 \times 10^{-3}\ s^{-1}$ [d]	$K_{h3} = 7.2 \times 10^{-3}$ M		
$k_{-5}/k_6 = 7.5 \times 10^2\ M^{-1}$	$k_{-5}/k_6 = 7.3 \times 10^2\ M^{-1}$ [d]	$k_{-5}/k_6 = 7.3 \times 10^2\ M^{-1}$ [d]			

[a] Reference 16. [b] This work. [c] Statistical factor was taken into account.[18] [d] At 40 °C.

constant could not be determined for this step. Step 2 and step 3 were exactly first order, and no further reaction was observed for at least a couple of hours.

The observed rate constants k_{obs2} and k_{obs3} for step 2 and step 3 in the reaction with 4-penten-1-ol increased linearly with increasing C_L, and the slopes of the plot of k_{obs2} vs C_L decreased with increasing $[H^+]$ (Figure 3a). The slope of the k_{obs3} vs C_L plot was constant with respect to $[H^+]$ (Figure 3b). Thus, the mechanism of the reaction of the HT dimer with 4-penten-1-ol is constructed as in Scheme 2, which is virtually the same as for the HH dimer reaction with 4-penten-1-ol.[16] According to the mechanism in Scheme 2,

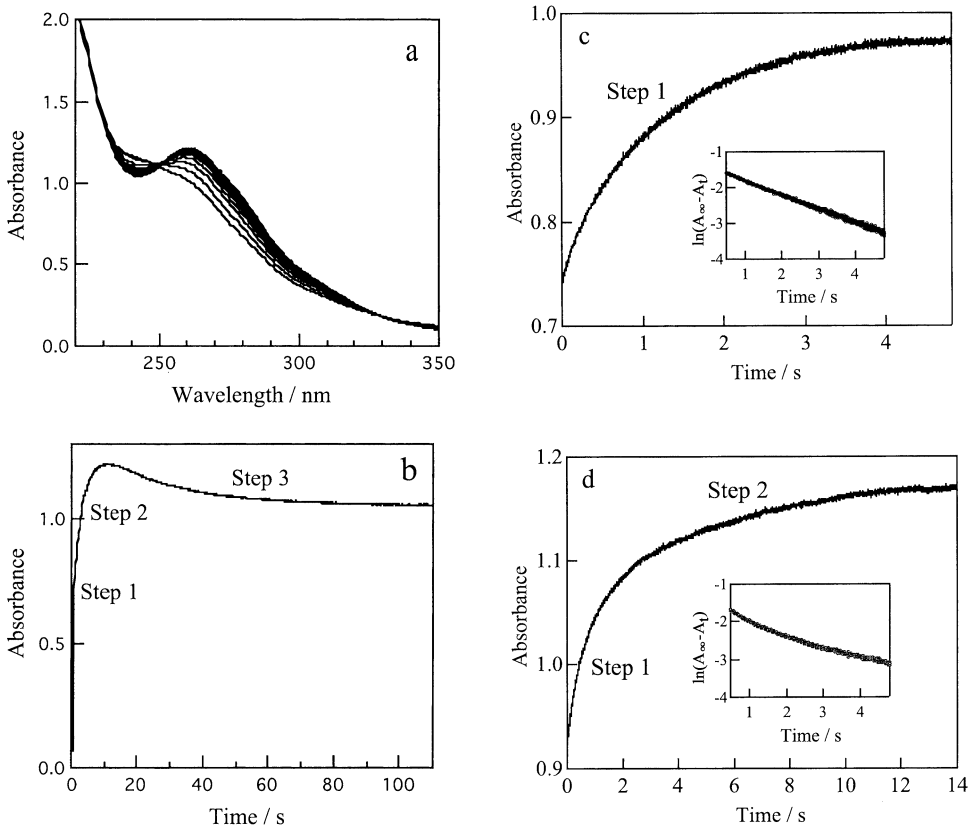

Figure 2. (a) Change of the UV−visible spectrum for the reaction of the HT dimer with 4-penten-1-ol, taken every 2 s at $I = 2.0$ M and 25 °C. $C_{HT} = 5 \times 10^{-5}$ M, $C_L = 7.02 \times 10^{-3}$ M, and $[H^+] = 1.66$ M. (b) The absorbance change with time at 265 nm in Figure 2a. (c) The absorbance change with time at 265 nm at higher C_L. $C_{HT} = 5 \times 10^{-5}$ M, $C_L = 1.42 \times 10^{-2}$ M, and $[H^+] = 1.66$ M. The inset shows the semilog plot of the data. (d) The absorbance change with time at 265 nm at lower C_L. $C_{HT} = 5 \times 10^{-5}$ M, $C_L = 4.74 \times 10^{-3}$ M, and $[H^+] = 1.66$ M. The inset shows the semilog plot of the data.

k_{obs2} and k_{obs3} are expressed as eqs 9 and 10, respectively, under the present conditions.

$$k_{obs2} = k_{f2}[L] = \frac{k_2[H^+] + k_2^{\#}K_{h2}}{[H^+] + K_{h2}}[L] \approx \left(k_2 + \frac{k_2^{\#}K_{h2}}{[H^+]}\right)[L] \quad (9)$$

$$k_{obs3} = k_{f3} + k_{d3}[L] = \frac{k_3K_{h3}}{[H^+] + K_{h3}} + k_{-3}[L] \approx k_{-3}[L] \quad (10)$$

The data in Figure 3 were successfully analyzed according to eqs 9 and 10 (see also Figure S6, Supporting Information). The rate constants in eqs 9 and 10 are given in Table 1.

The definite difference between the HH and HT reaction mechanisms is the reaction paths in step 2. Step 2 in Scheme S1 involves two paths, k_2 and k_3, whereas step 2 in Scheme 1 involves three paths, k_2, k_3, and $k_2^{\#}$.

In step 2 in Scheme 1, the reaction proceeds through k_2 and k_3 paths; in the k_2 path, direct substitution of the H_2O on the $Pt(N_4)$ with an olefin occurs, whereas the k_3 path includes a coordinatively unsaturated intermediate. In contrast, the reaction of the HH dimer with 4-penten-1-ol proceeds through k_2 and $k_2^{\#}$ paths (in Scheme S2 in Supporting Information, in which the reaction paths are essentially the same as for the present HT dimer in Scheme 2 as mentioned previously), and in the $k_2^{\#}$ path, OH^- on the $Pt(N_4)$ is substituted with the olefin. This difference of step 2 between Schemes 1 and S1 can be explained by the difference of the strength of the olefin π-coordination bond, i.e., the π bond between the olefin and the $Pt(N_2O_2)$ in aqua-π-olefin dimers is more effectively strengthened for *p*-styrenesulfonate than 4-penten-1-ol by accepting more electrons from the d orbitals of the $Pt(N_2O_2)$. This is facilitated by the electron-withdrawing benzenesulfonate group.[16] This more stable π-coordination means that the $Pt(N_2O_2)$ is in a more positive oxidation state for *p*-styrenesulfonate than 4-penten-1-ol in the aqua-π-olefin dimers. As a result, the $Pt(N_4)$ is less positive for *p*-styrenesulfonate, and the H_2O molecule on the $Pt(N_4)$ is less stable for *p*-styrenesulfonate and therefore the H_2O is released. This is the k_3 path. This difference of the reaction paths shows that the electronic state of the aqua-π-*p*-styrenesulfonate dimer is close to H_2O-$Pt^{II}(N_4)$-$Pt^{IV}(N_2O_2)$-π-*p*-styrenesulfonate, whereas that of the aqua-π-4-penten-1-ol is close to H_2O-$Pt^{III}(N_4)$-$Pt^{III}(N_2O_2)$-π-4-penten-1-ol. On the other hand, when the hydroxy-π-olefin dimers are compared, the electronic structure is reversed to HO-$Pt^{III}(N_4)$-$Pt^{III}(N_2O_2)$-π-*p*-styrenesulfonate and HO-$Pt^{II}(N_4)$-$Pt^{IV}(N_2O_2)$-π-4-penten-1-ol. This is the reason for the $k_2^{\#}$ path to exist only for π-4-penten-1-ol. Considering these flexible oxidation states of the two Pt atoms, it is understandable that the HT dimer in Scheme 1 has all the three paths in step 2, k_2, $k_2^{\#}$, and k_3, since the HT dimer is expected to have less delocalized electronic state compared to the HH dimers. All the Pt oxidation states mentioned above are only approximate

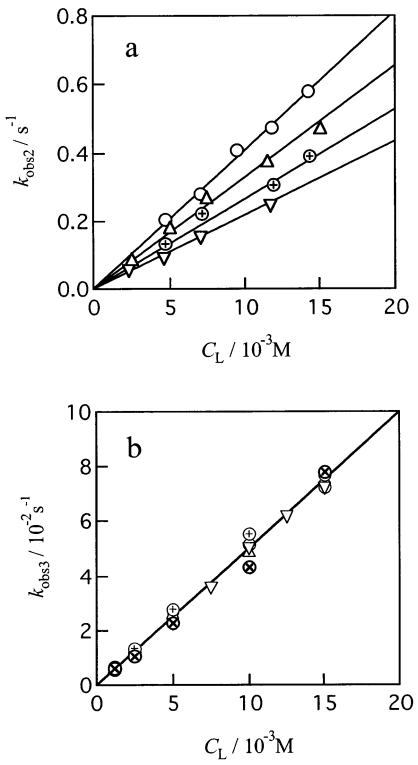

Figure 3. Dependence of the observed rate constants on C_L for the reaction of the HT dimer with 4-penten-1-ol at $I = 2.0$ M. (a) For step 2, at 25 °C and $[H^+]/M = 0.206$ (○), 0.411 (△), 0.822 (⊕), 1.66 (▽). (b) For step 3, at 25 °C and $[H^+]/M = 0.0100$ (○), 0.0401 (△), 0.201 (⊕), 0.401 (▽), 0.803 (⊗).

expressions to help understand how the electrons move along the Pt−Pt bond in each step. The expression H_2O-$Pt^{II}(N_4)$-$Pt^{IV}(N_2O_2)$-π-olefin does not mean that olefins can π-coordinate to Pt^{IV}. It only shows that the $Pt(N_2O_2)$ oxidation state would be higher than Pt^{III}.

The order of trans effect and/or influence of the olefin in the HT aqua-π-*p*-styrenesulfonate dimer in step 2 in Scheme 1 would be intermediate between the HH analogue in Scheme S1 and the HH aqua-π-4-penten-1-ol dimer (in step 2 in Scheme S2). In other words, the HT aqua-π-*p*-styrenesulfonate dimer has an intermediate character between the HH analogue and the HH aqua-π-4-penten-1-ol dimer, and therefore, step 2 in Scheme 1 has both k_3 and $k_2^{\#}$ paths. In accordance with this, in Table 1, K_{h2} (7.7×10^{-3} M) for the HT reaction with *p*-styrenesulfonate is ca. 20 times larger than that (3.8×10^{-4} M) for the HH reaction with *p*-styrenesulfonate, and is comparable to the value (6.3×10^{-3} M) for the HH reaction with 4-penten-1-ol. On the other hand, k_3 (0.70 s^{-1}) for the HT reaction with *p*-styrenesulfonate is comparable to k_3 (0.64 s^{-1}) for the HH reaction with *p*-styrenesulfonate. The rate constants of step 2 for the reactions of the HH amidato-bridged *cis*-diammineplatinum(III) dimer with halide ions are given in Table 2.[19] In this table, the reactions of the HH α-pyrrolidonato-bridged dimer and the pivalamidato-bridged dimer with Cl^- have only the k_2 path, and their values are of the order of 10^3. When the k_2 value is large as in this order, step 2 consists of solely the k_2 path. As the k_2 value decreases, the reaction path $k_2^{\#}$ or k_3 appears in addition to k_2, and this is the case for most of the

Table 2. The Rate Constants for Step 2 of the Reactions of the HH Amidato-Bridged *cis*-Diammineplatinum(III) Dimer with Halide Ions at $I = 2.00$ M and 25 °C[a]

ligand	bridging ligand	path	k [M^{-1} s^{-1}]
Cl^-	α-pyridonate[b]	k_2	$(5.50 \pm 0.10) \times 10^2$
		k_3[c]	3.1 ± 0.3
		k_{-3}/k_4[d]	$(3.7 \pm 0.5) \times 10^{-3}$
	α-pyrrolidonate	k_2	$(1.52 \pm 0.01) \times 10^3$
	pivalamidate	k_2	$(1.51 \pm 0.01) \times 10^3$
		k_{-2}[c]	$(8.66 \pm 0.24) \times 10^{-1}$
Br^-	α-pyridonate[b]	k_2	$(4.50 \pm 0.36) \times 10^2$
		k_3	4.4 ± 0.8
		k_{-3}/k_4[d]	$(3.7 \pm 0.8) \times 10^{-3}$
	α-pyrrolidonate	k_2	$(1.36 \pm 0.07) \times 10^2$
		k_3	1.39 ± 0.07
		k_{-3}/k_4[d]	$(7.73 \pm 0.93) \times 10^{-4}$
	pivalamidate	k_2	$(1.01 \pm 0.30) \times 10^2$
		k_{-2}[c]	$(1.25 \pm 0.46) \times 10^{-2}$
		$k_2^{\#}K_{h2}$[c]	$(8.52 \pm 0.81) \times 10^2$

[a] Reference 19. [b] Reference 17. [c] In s^{-1}. [d] In M.

systems in Table 2. When the k_2 value becomes further lower as in the present HT reactions with *p*-styenesulfonate ($k_2 = 8.5$ M^{-1} s^{-1}) and 4-penten-1-ol ($k_2 = 10$ M^{-1} s^{-1}), step 2 has three paths depending on the nature of the olefin in the aqua-π-olefin dimer. Thus, the paths involved in step 2 depend on the magnitudes of $k_2^{\#}K_{h2}$ and k_3 relative to k_2 in eq 6.

In step 3 in Scheme S1, a water molecule is coordinated on the $Pt(N_4)$ in the σ-complex, whereas no water molecule exists on the $Pt(N_4)$ in the σ-complex of the reaction with 4-penten-1-ol (Scheme S2). This difference was explained by the decreased electron-donating ability of the substituted alkyl group in the σ-complex in Scheme S1 due to the benzenesulfonate group, which reduces the electron localization in the dinuclear complex (X_1-$Pt^{IV}(N_2O_2)$-$Pt^{II}(N_4)$-X_2) to the less localized complex (X_1-$Pt^{III}(N_2O_2)$-$Pt^{III}(N_4)$-X_2).[16]

The K_{h3} of the HT dimer reaction with *p*-styrenesulfonate is substantially larger than that of the HH dimer in Table 1, even if the temperature difference is taken into account. In our previous report on the α-pyridonato-bridged HH dimer reaction with halide ion,[17] the first substitution occurs preferentially to the $Pt(N_2O_2)$ and the deprotonation of the coordinated water selectively takes place on the $Pt(N_4)$ (step 1 in Scheme S1), since the electrons are localized in the HH diaqua dimer as close to $[H_2O$-$Pt^{IV}(N_4)$-$Pt^{II}(N_2O_2)$-$OH_2]^{4+}$. This has been supported by the recent ^{195}Pt NMR measurement of the HH and HT diaqua α-pyridonato-bridged dimers; the chemical shifts are −1488 ppm ($Pt(N_4)$) and −2863 ppm ($Pt(N_2O_2)$) for the HH dimer, and −1766 ppm ($Pt(N_3O)$ for the HT dimer, with reference to $PtCl_6^{2-}$ (0 ppm).[22] The electron localization is also observed in the X-ray crystallography: in the HH dichloro α-pyrrolidonato-bridged dimer $[Cl$-$Pt(N_4)$-$Pt(N_2O_2)$-$Cl]^{2+}$,[21] the $Cl-Pt(N_2O_2)$ is longer than $Cl-Pt(N_4)$, which suggests that the electronic state is localized as $[Cl$-$Pt^{IV}(N_4)$-$Pt^{II}(N_2O_2)$-$Cl]^{2+}$.[21] On the contrary, the electron localization is in the opposite direction in the alkyl HH pivalamidato-bridged dimers, e.g., $[NO_3$-$Pt^{II}(N_4)$-$Pt^{IV}(N_2O_2)$-$CH_2CHO]^{2+}$,[20] due to the strong trans influence of the alkyl group. Similar inversion of the electron localiza-

(22) Unpublished results.

tion direction has been observed in the reaction of the HH pivalamidato-bridged diaqua complex with olefins to form the mono β-hydroxy alkyl dimer complex.[16] Analogously, in the π,σ-HH and HT dimers (π,σ-complexes), the electronic states would be [π-$Pt^{II}(N_4)$-$Pt^{IV}(N_2O_2)$-σ]$^{3+}$ in the HH dimer in Scheme S1 and [π-$Pt^{II}(N_3O)$-$Pt^{IV}(N_3O)$-σ]$^{3+}$ in the HT dimer in Scheme 1; the degree of electron localization would be more pronounced in the HH π,σ-complex. Therefore, the HH π,σ-complex would be more stable than the HT analogue, considering that Pt complexes in the lower oxidation states tend to form stable π-complexes. The fact that the K_{h3} value of the HT reaction with *p*-styrenesulfonate is larger than that of the HH dimer (Table 1) indicates that the energy difference between the π,π-complex (e.g., [π-Pt-(N_4)-$Pt(N_2O_2)$-π]$^{4+}$ in Scheme S1) and π,σ-complex is larger for the HT dimer. It follows therefore that the HH π,π-complex is more thermodynamically stable than the HT π,π-complex. All the synthetic and X-ray studies show that monoalkyl HH complexes have always the alkyl groups on the $Pt(N_2O_2)$, which suggests that the π to σ conversion by water attack occurs always to the $Pt(N_2O_2)$-π in the HH dimer, in other words, water attack occurs easier to the $Pt(N_2O_2)$-π than the $Pt(N_4)$-π, which means that the electronic states of $Pt(N_2O_2)$ and $Pt(N_4)$ in the HH π,π-complex are not equivalent and the π ligand on the $Pt(N_2O_2)$ is more positively charged than that on the $Pt(N_4)$, suggesting the localization of $Pt^{IV}(N_2O_2)$-$Pt^{II}(N_4)$. Considering that the two $Pt(N_3O)$ are equivalent in the HT π,π-complex, the water attack to the olefin in the π,π-complexes is expected to be faster in the order $Pt(N_2O_2)$-π > $Pt(N_3O)$-π > $Pt(N_4)$-π, i.e., HH > HT, though the rate constant of this step could not be measured.

The k_3 and K_{h3} values could not be determined for the HT dimer reaction with 4-penten-1-ol, because of the relation $k_3K_{h3}/([H^+] + K_{h3}) \ll k_{-3}[L]$ in eq 10 under the present experimental conditions. This is probably due to the very small K_{h3}.

Conclusion

The reactions of the HT α-pyridonato-bridged Pt^{III} dinuclear complex with olefins were basically the same as those of the HH α-pyridonato-bridged Pt^{III} dinuclear complex, except for step 2 in the reaction with *p*-styrenesulfonate. Step 2 in the HH dimer reaction consists of two paths (k_2 and k_3), whereas in the HT dimer reaction it consists of three paths (k_2, k_3, and $k_2^{\#}$). The difference can be qualitatively explained by the relative degree of electron localization in the HH and HT aqua-π-olefin complexes. The previous reactions of the HH amidato-bridged Pt^{III} dinuclear complexes with halide ions[19] and the present reactions show that the reaction proceeds via one of the four cases, i.e., (k_2), (k_2 and k_3), (k_2 and $k_2^{\#}$), and (k_2, k_3, and $k_2^{\#}$) in step 2 in the HH and HT dimer reactions, depending on the k_2 value relative to the other rate constants, and the nature of the coordinated axial ligand on the opposite $Pt(N_2O_2)$ or $Pt(N_3O)$ atom. In the more localized HH dimer, the hydroxide opposite to the π-*p*-styrenesulfonate is more stable than that in the HT dimer, and is not substituted with the second *p*-styrenesulfonate ion, i.e., the $k_2^{\#}$ path does not exist for the HH dimer, whereas it exists for the HT dimer. The difference is also explained by the more localized H_2O-$Pt(N_4)$-$Pt(N_2O_2)$-(*p*-styrenesulfonate) structure of the HH dimer, which more destabilizes the H_2O−$Pt(N_4)$ bond than in the HT dimer and the k_2 and k_3 paths become possible in step 2. Although the difference of the K_{h3} values of the HH and HT dimers shows only the energy difference of the π,π-complex and π,σ-complex in the HH and HT dimers, the HT π-$Pt(N_3O)$-$Pt(N_3O)$-σ state would be less stable than the HH π-$Pt(N_4)$-$Pt(N_2O_2)$-σ, and therefore the HT π-$Pt(N_3O)$-$Pt(N_3O)$-π would be also less stable than the HH π-$Pt(N_4)$-$Pt(N_2O_2)$-π dimer. The HT dimer is more stabilized by the nucleophilic attack of water to the π-olefin to become the π-$Pt(N_3O)$-$Pt(N_3O)$-σ complex. This seems the reason for the larger K_{h3} for the HT dimer. In this way, the comparison of the corresponding HH and HT dimers gives the idea about how the complexes stabilize their intermediates depending on the axial ligand, by redistributing the electrons along the Pt−Pt bond.

Experimental Section

Reagents. *cis*-$[Pt(NH_3)_2Cl_2]$ was prepared from $K_2[PtCl_4]$ (Tanaka Kikinzoku Kogyo K.K., Tokyo) according to Dhara's method.[23] Reagent grade α-pyridone (Kanto Chemical Co. Inc., Tokyo) and 4-penten-1-ol (Tokyo Chemical Industry Co. Ltd.) were purified as described previously.[16] Sodium *p*-styrenesulfonate (Tokyo Chemical Industry Co. Ltd.) and perchloric acid (60% UGR for trace analysis, Kanto) were used without further purification. Sodium perchlorate was prepared and purified according to the literature.[24] Head-to-tail $[(H_2O)(NH_3)_2Pt(\mu\text{-}C_5H_4NO)_2Pt(NH_3)_2(NO_3)](NO_3)_3\cdot 2H_2O$ (HT dimer) was prepared according to the literature.[1]

Measurements. Ionic strength was maintained at 2.00 M (M = mol dm^{-3}) with perchloric acid and sodium perchlorate. All the sample solutions were prepared by using twice distilled water just before measurement. Spectrophotometric measurements were performed by using the same apparatus as described previously.[16] Rate constants were measured by monitoring the absorbance change at 350 nm for the reaction of the HT dimer with sodium *p*-styrenesulfonate and at 265 nm for the reaction with 4-penten-1-ol, as a function of time after mixing the solutions of the dimer and the olefin. Under the conditions that the concentration of the olefin (C_L) is in large excess over that of the dimer complex (C_{HT}), the reaction was found to consist of several consecutive first-order steps. The rate constants were determined as described previously.[16]

The ^{1}H NMR spectra were recorded on a JEOL Lambda 270 spectrometer. The chemical shift was referenced to TMA (tetramethylammonium perchlorate, 3.190 ppm to TMS).

Acknowledgment. Financial Support from the 21COE "Practical Nano-Chemistry" from MEXT, Japan, is gratefully acknowledged.

Supporting Information Available: Tables S1 and S2, providing observed rate constants, Schemes S1 and S2, showing reaction mechanisms, and Figures S1−S6, presenting spectrophotometric, kinetic, and NMR data. This material is available free of charge via the Internet at http://pubs.acs.org.

IC034599Q

(23) Dhara, S. C. *Indian J. Chem.* **1970**, *8*, 193.
(24) Funahashi, S.; Haraguchi, K.; Tanaka, M. *Inorg. Chem.* **1977**, *16*, 1349.